analytical chemistry

pubs.acs.org/ac Article

Enrichment and Liquid Chromatography–Mass Spectrometry Analysis of Trastuzumab and Pertuzumab Using Affimer Reagents

Oladapo Olaleye, Baubek Spanov, Robert Ford, Natalia Govorukhina, Nico C. van de Merbel, and Rainer Bischoff*

Cite This: *Anal. Chem.* 2021, 93, 13597–13605 Read Online

ACCESS | Metrics & More | Article Recommendations | Supporting Information

ABSTRACT: Trastuzumab and pertuzumab are monoclonal antibodies used in the treatment of human epidermal growth factor receptor-2 (HER2)-positive breast cancer. Therapeutic proteins may undergo chemical modifications that may affect the results of bioanalytical assays, as well as their therapeutic efficacy. Modifications may arise during production and storage, as well as after administration to patients. Studying in vivo biotransformation of monoclonal, therapeutic antibodies requires their enrichment from plasma to discriminate them from endogenous antibodies, as well as from other plasma proteins. To this end, we screened Affimer reagents for selectivity toward trastuzumab or pertuzumab. Affimer reagents are alternative binding proteins possessing two variable binding loops that are based on the human protease inhibitor stefin A or phytocystatin protein scaffolds. Affimer reagents were selected from an extensive library by phage display. The four best-performing binders for each therapeutic antibody were prioritized using a microtiter plate-based approach combined with liquid chromatography–mass spectrometry (LC–MS) in the selected reaction monitoring (SRM) mode. These Affimer reagents were immobilized via engineered 6-His or Cys tags to Ni^{2+}- or maleimide beads, respectively. Recovery values of 70% and higher were obtained for both trastuzumab and pertuzumab when spiked at 100, 150, and 200 μg/mL concentrations in human plasma followed by trypsin digestion in the presence of 0.5% sodium deoxycholate and 10 mM dithiothreitol (DTT). Notably, the maleimide beads showed undetectable unspecific binding to endogenous immunoglobulin G (IgGs) or other plasma proteins when analyzed by sodium dodecyl sulfate-polyacrylamide gel electrophoresis (SDS-PAGE). The enrichment method was applied to samples from stress tests of the antibodies at 37 °C to mimic in vivo conditions.

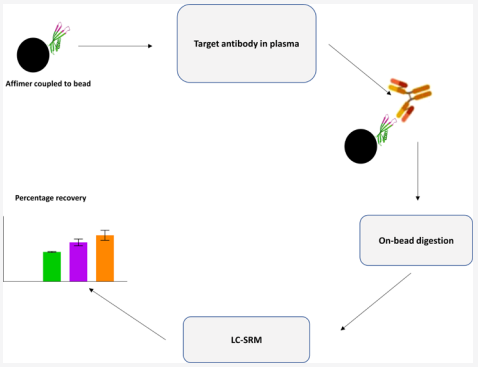

INTRODUCTION

Trastuzumab and pertuzumab are monoclonal antibodies employed in the treatment of human epidermal growth factor receptor-2 (HER2)-positive breast cancer.[1−3] They are humanized antibodies produced using recombinant DNA technology by placing complementary determining regions (CDRs) of mouse antibodies into human framework regions and constant parts.[4] Trastuzumab binds to domain IV of the extracellular part of HER2[5] and prevents HER2 dimerization,[3] while pertuzumab adheres to extracellular domain II[6] and inhibits HER2 heterodimerization with other receptors of the HER family.[3] Trastuzumab also inhibits heterodimerization although not as effectively as pertuzumab.[7] Both antibodies interact with Fc-γ receptors (e.g., on natural killer cells) to induce antibody-dependent cell-mediated cytotoxicity (ADCC) against tumor cells.[3,8]

Biotransformation refers to modifications that occur in biopharmaceuticals after they have been administered to patients.[9] These modifications, such as oxidations or deamidations, may result in reduced half-life, decreased target binding, increased immunogenicity, or reduced affinity for Fc-γ receptors.[10] For example, asparagine deamidation in a human growth hormone-releasing factor was shown to result in reduced efficiency[11] and aspartic acid isomerization in trastuzumab caused the loss of antiproliferative activity in an assay using a breast cancer cell line.[12] Modifications may also affect the results of bioanalytical assays leading to variable and possibly erroneous results. For example, the deamidation of Asn-55 in the heavy chain of trastuzumab leads to the loss of recognition by anti-idiotypic antibodies in a validated enzyme-linked immunosorbent assay (ELISA).[13] Deamidation results in the formation of carboxylic acid derivatives of asparagine and glutamine residues due to the hydrolysis of the side-chain amides.[14] This process begins with the formation of a succinimide intermediate and results in two isobaric forms, one containing aspartic acid and the other isoaspartic acid. Deamidation has been reported to occur at a faster rate at asparagine residues and to be strongly

Received: July 5, 2021
Accepted: September 7, 2021
Published: September 28, 2021

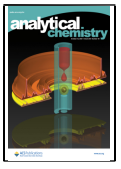

https://doi.org/10.1021/acs.analchem.1c02807
Anal. Chem. 2021, 93, 13597−13605

affected by the sequence and structural context.[15,16] Bults et al.[13] reported the deamidation of Asn-55 in one of the CDRs of trastuzumab by detecting the corresponding signature peptides containing aspartic acid and isoaspartic acid, as well as a small amount of the succinimide intermediate in the plasma of patients receiving the drug.

The complexity of clinical samples, like blood serum or plasma, requires a means to successfully isolate proteins of interest for further analysis, for example, to study their biotransformation.[17] Affinity enrichment involves the use of capturing agents or binders to selectively bind these proteins.[18] Antibodies are most widely used for this purpose due to their availability, their use in ligand binding assays, and the often high affinity and specificity for their targets.[19,20] However, antibodies come with a number of challenges such as an expensive and lengthy production process, possible cross-reactivity,[21] and issues with batch-to-batch variability.[20] To address these limitations, other antibody-based binders such as fragment antigen-binding (Fab) and single-chain variable fragments (scFv) have been designed,[22] as well as a range of nonantibody-based binders, comprising aptamers, avimers, knottins, DARPins, and Affimer reagents.[20,23] Affimer reagents are a group of alternative binding proteins, which possess two variable binding loops inserted into the human protease inhibitor stefin A or phytocystatin protein scaffolds. The structure of an affimer protein consists of four β sheets and an α helix.[23] The two variable binding loops contain about nine amino acids each, which can be changed at random to bind different targets using phage display technology.[23] Affimer reagents possess similar affinity and specificity as antibody-based binders but are smaller, produced more easily in bacterial expression systems, stable at high temperatures, and over a wide pH range.[23] Affimer reagents have been used in different applications such as molecule detection, biosensing, and cell imaging with promising results.[20,24−29] An interesting study involving Affimer reagents targeted against four monoclonal antibodies in a sandwich ELISA produced results that met Food and Drug Administration (FDA) requirements for accuracy and precision when compared to commercial, antibody-based assay kits.[24]

Here, we describe an approach to enrich trastuzumab and pertuzumab from human plasma in combination with mass spectrometry analysis. Affimer reagents were initially selected from a library of about 10^{10} clones based on their capacity to specifically bind to trastuzumab or pertuzumab without cross-reactivity to other human immunoglobulin G (IgGs). They were further prioritized using a microtiter plate-based enrichment approach followed by liquid chromatography−mass spectrometry (LC−MS) analysis in the selected reaction monitoring (SRM) mode. The best-performing Affimer reagents were transferred to a bead-based enrichment method to obtain sufficient amounts of the therapeutic antibodies for further study. The bead-based enrichment procedure was optimized with spiked-in therapeutic antibodies in human plasma and validated in terms of specificity and notably recovery. The enrichment method was applied to forced stability studies trying to mimic in vivo conditions. The ability to apply this method to clinical samples of patients receiving trastuzumab and pertuzumab as therapy for HER2-positive breast cancer will provide a means to further analyze the possible modifications that these antibodies might undergo in vivo.

METHODS

Selection of Signature Peptides and Trypsin Digestion. To quantify the amount of trastuzumab and pertuzumab that was enriched by a given Affimer reagent, signature peptides were selected for each antibody. The signature peptide for trastuzumab (DrugBank 5.0; identifier DB00072)[30] was chosen according to Bults et al.[13] For pertuzumab, an in silico digestion was performed via mMass[31] on the pertuzumab sequence (DrugBank 5.0; identifier DB06366)[30] to generate peptides expected after trypsin digestion. The peptides were subjected to the basic local alignment search tool (BLAST version 2.2.29)[32] against the SwissProt database (UniProt release 2018_07) to assure that they do not occur in any other human protein.

Pertuzumab was digested overnight at 37 °C and 700 rpm with a digestion mixture containing Milli-Q water, 250 mM Tris−HCl, pH 7, 4 mg/mL porcine trypsin (in 1 mM HCl), and dimethyl sulfoxide (DMSO) (ratio 23:8:8:1), respectively, in peptide mapping experiments to make sure that the selected signature peptide was detectable by LC−MS analysis using system 1 (see the following section). The SIL standards of both peptides were directly infused into system 1 and subjected to LC−MS to choose the optimal conditions for fragmentation. The three most intense fragment ions were selected for further analysis. The sum of the peak areas of the three fragment ions was used to quantify each peptide (see Table 1 for details).

Table 1. Selected Signature Peptides and Their Corresponding Fragment Ions as Used for the Quantification of Trastuzumab and Pertuzumab by LC−MS

	peptide precursor ion	peptide fragment ions	collision energy
trastuzumab (heavy chain)	^{68}FTISADTSK^{76} (485.2^{2+})	335.2^{1+}(y3), 608.3^{1+}(y6), 721.4^{1+}(y7)	23
pertuzumab (heavy chain)	^{68}FTLSVDR^{74} (419.2^{2+})	476.2^{1+}(y4), 589.3^{1+}(y5) 690.4^{1+}(y6)	21
trastuzumab SIL	FTISADTSK* (489.2^{2+})	343.2^{1+}(y3), 616.3^{1+}(y6), 729.4^{1+}(y7)	23
pertuzumab SIL	FTLSVDR* (424.2^{2+})	486.2^{1+}(y4), 599.3^{1+}(y5) 700.4^{1+}(y6)	21

LC−MS Analysis. Quantitative mass spectrometric data were acquired using two different systems (system 1 and system 2) and exported for visualization to GraphPad Prism 6 (GraphPad Software, Inc., San Diego, CA). Shotgun proteomics data were acquired using system 3.

System 1 consisted of an Eksigent ekspert nanoLC 425 and a quadrupole-time-of-flight (QTOF) mass spectrometer (Triple TOF 6600; Sciex, Framingham, MA). This system was used during the microtiter plate-based screening process for affimer prioritization. Chromatographic separation was performed at 35 °C using a Luna Omega column (3 μm polar C18 particles, 100 Å pore size, 150 × 0.3 mm, part. no. 00F-4760-AC, Phenomenex, Utrecht, The Netherlands) with 0.1% formic acid (FA) in water as mobile phase A and 0.1% FA in acetonitrile (ACN) as mobile phase B at 5 μL/min with a 6 min linear gradient from 3 to 35% B, after which the column was cleaned (2 min at 80% B) and equilibrated (1 min at 3% B). Mass spectrometric settings were as follows: ion source gas 1 (GS1) 10, ion source gas 2 (GS2) 20, curtain gas (CUR) 25, temperature (TEM) 100, ionspray voltage floating (ISVF)

https://doi.org/10.1021/acs.analchem.1c02807
Anal. Chem. 2021, 93, 13597−13605

4500, and declustering potential (DP) 80. The system was run using Sciex Analyst TF software (version 1.8). Sciex Multiquant software (version 2.0) was used for data processing. The processed data were then exported for visualization in GraphPad Prism 8 (GraphPad Software, Inc., San Diego, CA).

System 2 consisted of an ACQUITY M-Class UPLC and a XEVO TQ-S triple quadrupole mass spectrometer (Waters, Milford, MA). This system was used while setting up the bead-based enrichment method and for the subsequent quantitative analyses. Chromatographic separation was performed at 60 °C using a Luna Omega column (3 μm polar C18 particles, 100 Å pore size, 150 × 1.0 mm, part. no. 00D-4742-A0, Phenomenex, Utrecht, The Netherlands) with 0.1% FA in water as mobile phase A and 0.1% FA in ACN as mobile phase B at 50 μL/min with an 8 min linear gradient from 10 to 18% B, after which the column was cleaned (2.9 min at 90% B) and equilibrated (1 min at 10% B). Mass spectrometric analysis was performed using the following conditions: electrospray ionization (ESI) positive, precursor ion, and fragment ion windows at unit mass resolution (0.7 amu), span 0.2, capillary voltage 3.5 kV, cone voltage 30 V, source offset 50 V, source temperature 120 °C, cone gas at 150 L/h, sheath gas at 0.2 bar, and collision gas at 0.15 mL/min. The MS system was operated under the Waters MassLynx software suite (version 4.1), and the TargetLynx module of this package was used for data processing. The processed data were exported for visualization in GraphPad Prism 8 (GraphPad Software, Inc., San Diego, CA).

System 3 consisted of an Ultimate 3000 nano-HPLC system coupled online to a Q-Exactive-Plus mass spectrometer with a NanoFlex source equipped with a stainless steel emitter (Thermo Fisher Scientific, Bremen, Germany). This system was used for shotgun proteomics analyses of nonspecifically bound proteins. Samples were loaded onto an Acclaim PepMap100, 5 μm, 100 Å, 300 μm i.d. × 5 mm trapping microcolumn (Dionex, Sunnyvale California; part no. 160454) in 0.1% FA at a flow rate of 20 μL/min. Peptides were eluted to an Acclaim PepMap100, C18, 2 μm, 100 Å, 75 μm i.d. × 50 cm, nanoViper column (Dionex; part no. 164942). Chromatographic separation was performed using 0.1% FA in water as mobile phase A and 0.1% FA in ACN as mobile phase B at 300 nL/min with a 60 min linear gradient from 2 to 50% B, after which the column was cleaned (5 min at 85% B) and equilibrated (15 min at 2% B). Mass spectrometric analysis was done in the data-dependent acquisition mode by choosing the top-15-most abundant precursor ions from survey scans (300−1650 Th) for fragmentation with a dynamic exclusion time of 20 s. Other settings were higher-energy collisional dissociation (HCD) fragmentation with a target value of 2×10^4 ions determined with a predictive automatic gain control, a precursor isolation window of 1.8 Da, an MS1 survey scan resolution of 70 000 at m/z 200, a spectral resolution of 17 500 at m/z 200 with a maximum ion injection time of 50 ms, a normalized collision energy (NCE) of 28, an S-lens RF level of 60, and a capillary temperature of 250 °C. Data were analyzed using the Peaks10 Studio software package (Bioinformatics Solutions Inc., Waterloo, Ontario, Canada) and searched against the Human Uniprot/Swissprot database (UniProt release 2020_03, 20 348 entries).

The raw mass spectrometry data involving the experiment that studies the nonspecifically bound plasma proteins to the beads have been deposited with the ProteomeXchange Consortium via the PRIDE partner repository with the data set identifier PXD027103.

RESULTS AND DISCUSSION

Prioritization of Affimers Using a Microtiter Plate-Based Format. To select the most suitable Affimer reagents for the enrichment of trastuzumab and pertuzumab, 16 antitrastuzumab and 18 antipertuzumab affimers were coated on microtiter plates and used to capture increasing amounts of trastuzumab and pertuzumab from both phosphate-buffered saline (PBS) and 50% human plasma. The amounts studied were 75, 150, 300, 750, and 1500 ng, which corresponds to 0.75, 1.5, 3, 7.5, and 15 μg/mL, respectively. A blank sample with no coated affimer was included to investigate the unspecific binding of the antibodies to the microtiter plates. HER2, which is the target protein for both antibodies, was used as a positive control and three antipertuzumab affimers were included in experiments targeting trastuzumab as negative controls to evaluate cross-reactivity and vice versa for pertuzumab. The captured antibodies were quantified by LC−MS in the SRM mode on system 1 using specific signature peptides. Figure S1 (Supporting Information) shows the results for trastuzumab and pertuzumab (panels A and C in PBS and panels B and D in 50% human plasma, respectively). Results are presented as peak area ratios between the antibody-derived signature peptides and the added stable-isotope-labeled peptide standards. These values were translated (using Table S1, Supporting Information) into percentages representing the overall recovery of the entire enrichment process including trypsin digestion, as detailed in Table S2 (Supporting Information). It is interesting to note that only 1−2% of the added antibodies are captured with this approach in plasma due to the small surface area of the microtiter plate wells favoring high-affinity binders over nonspecifically binding proteins.

The antibody-derived peptide signals observed in PBS were higher than in 50% plasma, suggesting interference from plasma proteins. The blanks and negative controls showed little or no signal, which suggests that there is little unspecific binding or cross-reactivity. The signals from HER2 in the case of trastuzumab (Figure S1A,B, Supporting Information) are considerably higher than those obtained for pertuzumab (Figure S1C,D, Supporting Information), which is consistent with the findings of Fuentes et al.[33] and Lua et al.,[34] who reported that trastuzumab has a higher affinity for HER2 than pertuzumab. Based on the signal intensity and a need to enrich the therapeutic antibodies from plasma, we selected the antitrastuzumab affimers T6, T11, T12, and T15 and the antipertuzumab affimers P3, P7, P9, and P17 for further studies.

Enrichment Using a Bead-Based Format. To enrich larger amounts of the therapeutic antibodies for further studies, we transferred the microtiter plate-based format to a bead-based format. To this end, we studied two different immobilization approaches, one based on the 6-His-tag and the other on the single Cys that were engineered into the affimer sequences at the C-terminus. Immobilization via the His-tag was based on Ni^{2+} ions that were chelated to the beads via a nitrilotriacetic acid (NTA) group. This is a noncovalent, reversible immobilization approach since the binding between affimers and the beads can be broken by adding a competing chelating agent like imidazole to the mobile phase or by shifting the pH into the slightly acidic range. This is a rather straightforward immobilization approach requiring no additional chemistry. The bead system for immobilization via the Cys residue contained maleimide groups, which form a covalent thioether bond with the affimer. This way

https://doi.org/10.1021/acs.analchem.1c02807
Anal. Chem. 2021, 93, 13597−13605

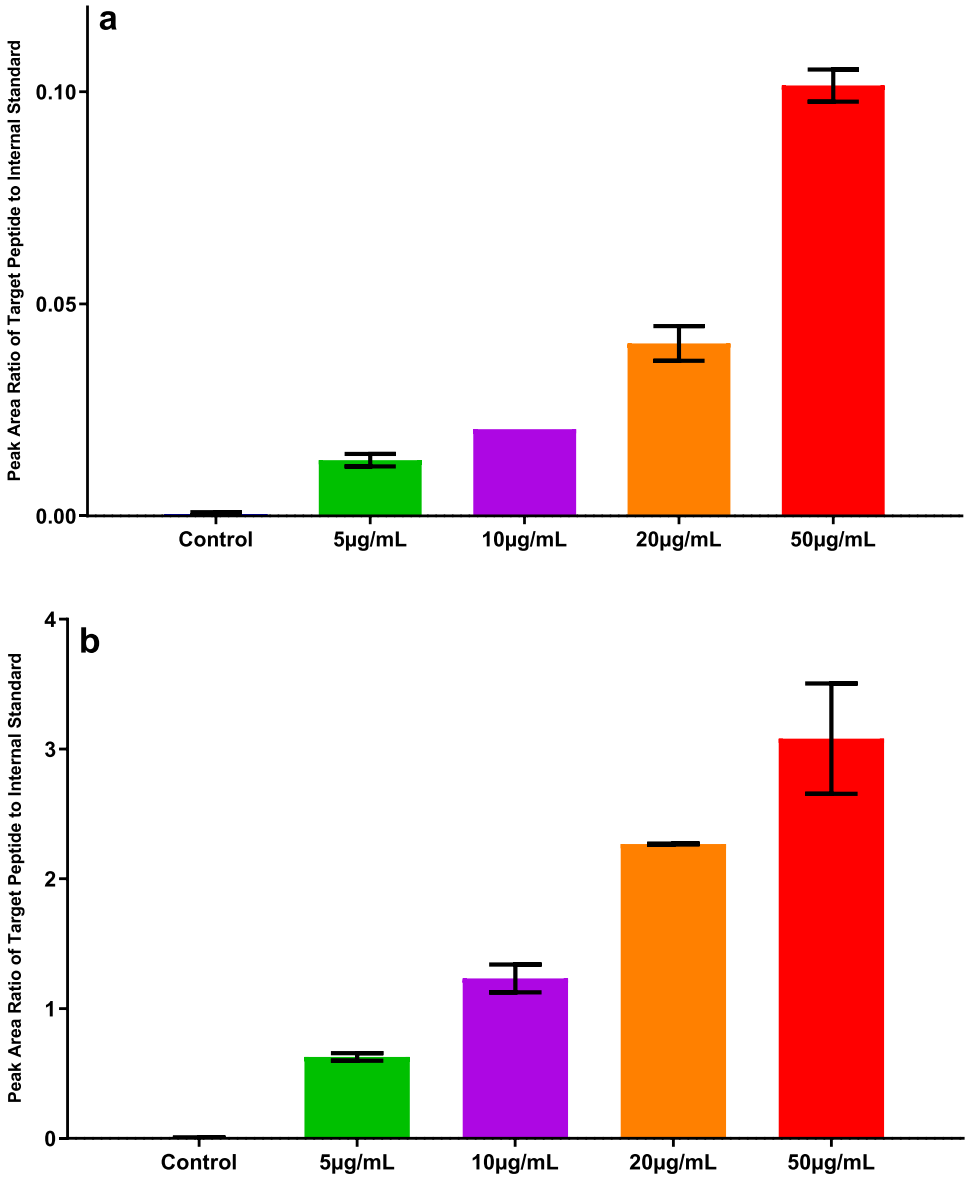

Figure 1. Evaluation of Ni^{2+} beads coupled with 1.5 μg of affimers T11 (a) and P7 (b) for the enrichment of trastuzumab (a) and pertuzumab (b) in 50% plasma, respectively. The peak area ratios between the antibody-derived signature peptides (FTISADTSK and FTLSVDR) and their respective stable-isotope-labeled peptide standards (n = 3) are represented. Beads with no affimer were used as control.

of immobilizing the affimer allows for more stringent washing and elution conditions.

Both bead systems were first studied for unspecific binding to trastuzumab and pertuzumab, as well as to other plasma proteins, as this might interfere with specific enrichment of the target therapeutic antibodies. To this end, beads (not coupled to affimers) were incubated with different concentrations of trastuzumab and pertuzumab in 50% plasma followed by on-bead digestion with trypsin. The maleimide beads were blocked with cysteine before incubation in plasma to avoid nonspecific binding via free SH-groups in other proteins (see the Methods section), while the Ni^{2+} beads did not require a blocking step. LC−MS analysis (system 2) showed that the signature peptides for trastuzumab or pertuzumab were not detected when incubated with beads that did not contain Affimer reagents at any of the studied concentrations (5−50 μg/mL), implying that the beads do not bind the antibodies nonspecifically in plasma. Shotgun proteomics analysis (system 3) showed, however, that an average of 110 plasma proteins was identified for the Ni^{2+} beads with at least two unique peptides and 116 proteins for the maleimide beads indicating some nonspecific binding, while analysis by sodium dodecyl sulfate-polyacrylamide gel electrophoresis (SDS-PAGE) showed nonspecific binding only in the case of the Ni^{2+} beads but not for the maleimide beads (see Figure S2, Supporting Information).

For initial experiments, 10 μL of Ni^{2+} beads was coupled to 1.5 μg of affimer T11 for trastuzumab and affimer P7 for pertuzumab based on the results of the microtiter plate-based prioritization in 50% plasma. Figure 1 shows the peak area ratios between the respective antibody-derived signature peptides and the added stable-isotope-labeled peptide standards for trastuzumab (a) and pertuzumab (b).

The measured peak area ratios indicate that the recovery of pertuzumab was considerably higher than that of trastuzumab. Since the same result was obtained with the maleimide beads (results not shown), it is unlikely that enrichment itself was the

https://doi.org/10.1021/acs.analchem.1c02807
Anal. Chem. 2021, 93, 13597−13605

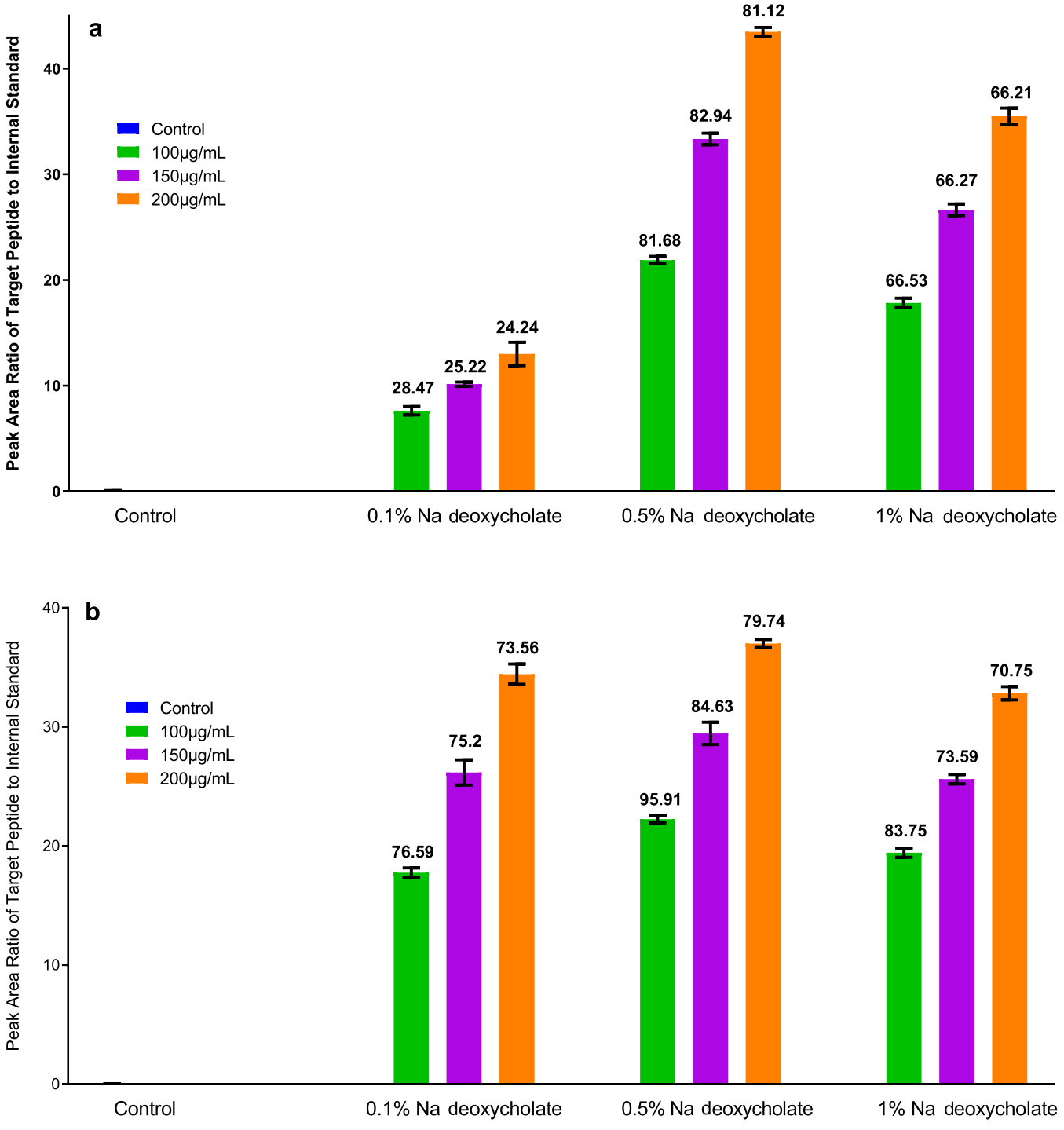

Figure 2. Evaluation of the effect of different concentrations of sodium deoxycholate on the on-bead trypsin digestion of trastuzumab (a) and pertuzumab (b). 40 μL of Ni^{2+} beads were coupled to 6 μg of affimers T11 (a) and P7 (b) for the enrichment of the antibodies from 50% plasma at 100, 150, and 200 μg/mL. Peak area ratios between the respective antibody-derived signature peptides (FTISADTSK and FTLSVDR) and the corresponding stable-isotope-labeled peptide standards are shown as readouts. Percentage recoveries are provided above each bar (n = 3). Beads with no affimer were used as control.

factor limiting recovery for this therapeutic antibody. Using the other three prioritized antitrastuzumab affimers T6, T12, and T15 coupled to Ni^{2+} beads did not lead to higher recoveries, further supporting this hypothesis (Figure S3, Supporting Information). That enrichment itself was not limiting recovery was further corroborated by analyzing the enriched fraction from the Ni^{2+} beads by gel electrophoresis, which showed clear bands for enriched trastuzumab that were comparable to pertuzumab (Figure S2, Supporting Information).

Optimization of the Digestion Procedure. Since enrichment of trastuzumab did not seem to be the limiting factor for recovery, we studied whether an incomplete release of the antibody-derived signature peptide during trypsin digestion could be a reason for the low signal. It is known that antibodies of the IgG family are rather resistant to trypsin digestion unless

https://doi.org/10.1021/acs.analchem.1c02807
Anal. Chem. 2021, 93, 13597−13605

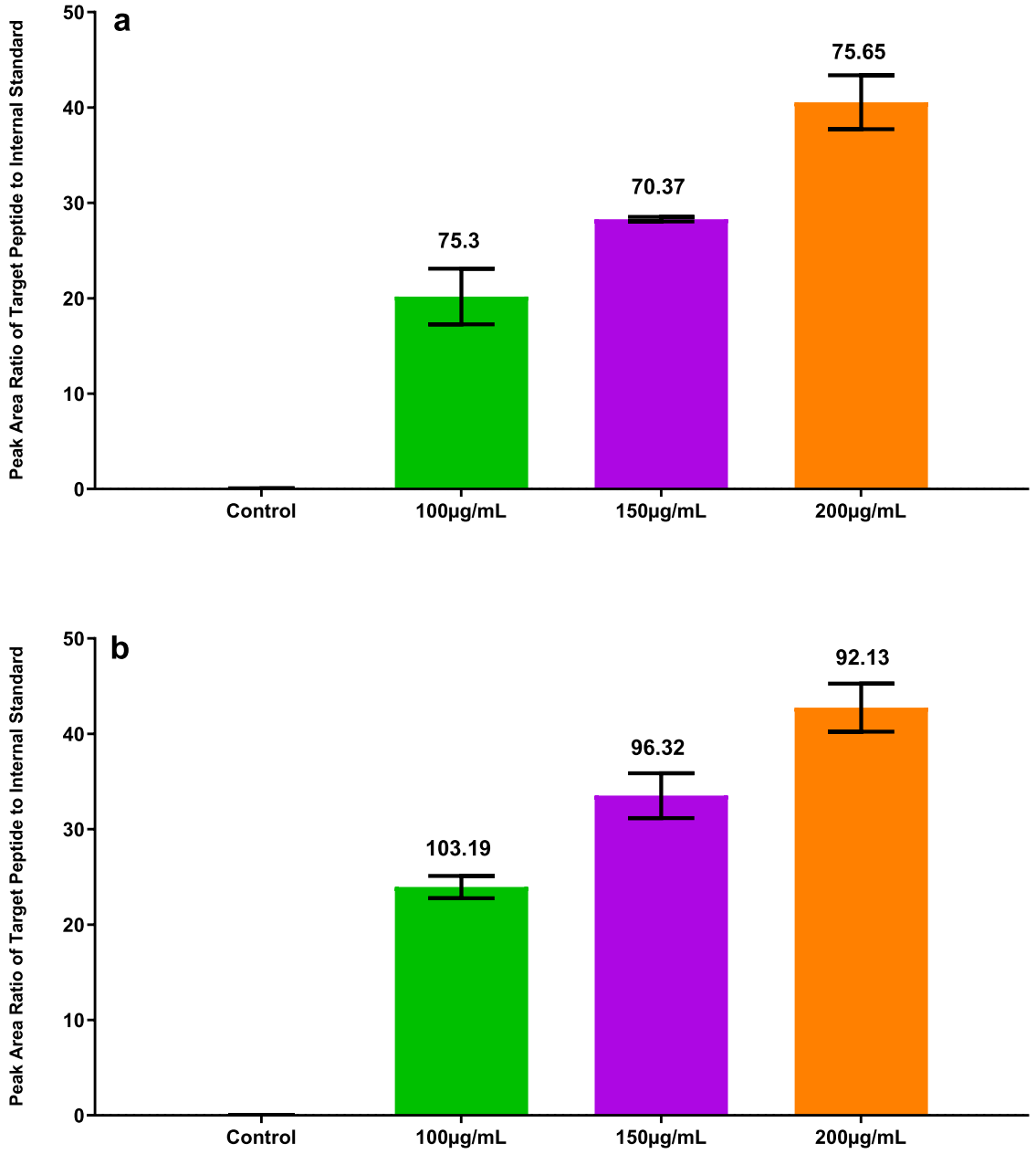

Figure 3. Evaluation of the maleimide bead enrichment of trastuzumab (a) and pertuzumab (b) in 50% plasma. 40 μL of maleimide beads were coupled to 12 μg of affimers T11 (a) and P7 (b) for the enrichment of the antibodies from 50% plasma at 100, 150, and 200 μg/mL showing peak area ratios between the respective antibody-derived signature peptides (FTISADTSK and FTLSVDR) and the corresponding stable-isotope-labeled peptide standards. Percentage recoveries are provided above each bar (n = 3). Beads with no affimer were used as control.

denatured;[35] 0.1% RapiGest[36] and 0.1 or 1% sodium deoxycholate[37] were therefore added to the samples after enrichment prior to digestion together with the reducing agent dithiothreitol (DTT) in 50 mM Tris−HCl, pH 7. Twenty microliters of Ni^{2+} beads were coupled to 3 μg of affimers T11 and P7 for the enrichment of 5, 10, 20, 50, 100, 150, and 200 μg/mL of trastuzumab and pertuzumab spiked in 50% plasma, respectively. This concentration range covers the concentrations observed in the plasma of patients treated with a combination of trastuzumab and pertuzumab (Bults et al., unpublished data). The peak area ratios between the measured signature peptides and the added stable-isotope-labeled peptide standards for trastuzumab and pertuzumab were determined (see Figure S4, Supporting Information) in comparison to beads without Affimer reagents that were incubated in 50% plasma containing the same concentration range of both antibodies as control.

The addition of surfactants and reduction with DTT significantly improved the release of the signature peptide for trastuzumab, as well as for pertuzumab, albeit to a lesser extent. It is interesting to note that the signature peptide for pertuzumab was more efficiently released in the absence of surfactants than for trastuzumab, although both antibodies have high overall similarity in their respective amino acid sequences (see Figure S5, Supporting Information). This probably relates to the location of the respective signature peptide in the antibody structure and its accessibility to trypsin. Sodium deoxycholate increased recovery dramatically in the case of trastuzumab, while 0.1% RapiGest worked best for pertuzumab. Recoveries of pertuzumab at 100, 150 and 200 μg/mL were lowest in 1%

https://doi.org/10.1021/acs.analchem.1c02807
Anal. Chem. 2021, 93, 13597−13605

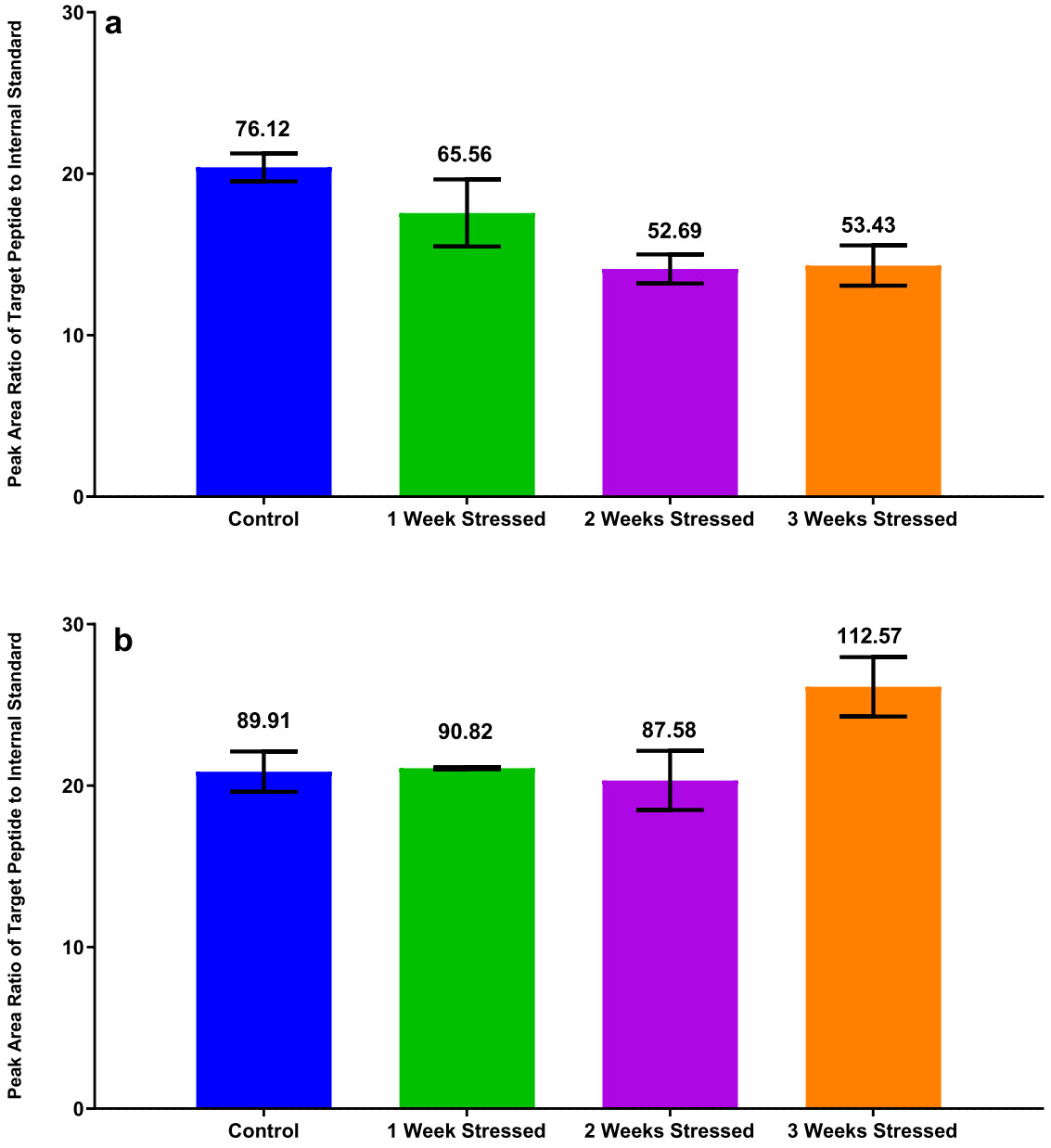

Figure 4. Evaluation of the enrichment of stressed trastuzumab (a) and pertuzumab (b) incubated in PBS, pH 7.4 at 37 °C at 100 ug/mL and spiked in 50% plasma. 40 μL of Ni^{2+} beads were coupled to 6 μg of affimers T11 (a) and P7 (b) for the enrichment of the antibodies showing peak area ratios between the respective antibody-derived signature peptides (FTISADTSK and FTLSVDR) and the corresponding stable-isotope-labeled peptide standards. Percentage recoveries are provided above each bar (n = 3). Nonstressed antibodies at 100 μg/mL in 50% plasma served as controls.

sodium deoxycholate when compared to those of 0.1% RapiGest or 0.1% sodium deoxycholate. In contrast, the release of the signature peptide from trastuzumab at the same concentrations was highest in 1% sodium deoxycholate when compared to that in 0.1% RapiGest or 0.1% sodium deoxycholate. This suggests that the best conditions for on-bead digestion for quantifying trastuzumab and pertuzumab based on the specified signature peptides may be different. To avoid having to use different digestion conditions, we further adjusted the concentration of sodium deoxycholate focusing on the higher concentrations of 100, 150, and 200 μg/mL. Concentrations of sodium deoxycholate of 0.1, 0.5, and 1% along with 10 mM DTT were added to the beads prior to digestion. To ensure that the capacity of the Ni^{2+} beads was not limiting at these elevated concentrations, we increased the bead volume to 40 μL coupled to 6 μg of affimer.

Sodium deoxycholate at 0.5% resulted in recoveries of 80−95% for both antibodies based on the release of the respective signature peptides at clinically relevant concentrations (Figure 2).

Since high levels of recovery were obtained for the Ni^{2+} beads, the process was transferred to the maleimide beads. Forty microliters of maleimide beads were coupled overnight to 12 μg of affimers T11 and P7 for the enrichment of trastuzumab and pertuzumab, respectively, from 50% plasma. After the enrichment process, the beads were incubated in 0.5% sodium deoxycholate and 10 mM DTT prior to digestion. Figure 3 shows the peak area ratios between the respective signature peptides and the added stable-isotope-labeled peptide standards for trastuzumab (a) and pertuzumab (b), as well as the respective recoveries in 0.5% sodium deoxycholate. While recovery is always higher than 70%, pertuzumab gives better

https://doi.org/10.1021/acs.analchem.1c02807
Anal. Chem. 2021, 93, 13597−13605

recoveries than trastuzumab when using the maleimide beads. This may still be due to the fact that the signature peptide of pertuzumab is more easily released than that of trastuzumab.

Stress Test of Trastuzumab and Pertuzumab. To understand the effect of possible modifications on Affimer reagent binding to trastuzumab and pertuzumab, both antibodies were incubated in PBS, pH 7.4 at 37 °C for 1, 2, and 3 weeks to mimic the conditions in a patient who receives the drug. Stressed antibody preparations were spiked in 50% plasma at a concentration of 100 μg/mL and 40 μL of Ni^{2+} beads that were coupled to 6 μg of affimers T11 and P7 were used for the enrichment of trastuzumab and pertuzumab, respectively. Nonstressed trastuzumab and pertuzumab at 100 μg/mL in 50% plasma served as controls. Figure 4 shows the peak area ratios between the respective signature peptides and the added stable-isotope-labeled peptide standards for trastuzumab (a) and pertuzumab (b) at the different time points.

While trastuzumab shows a significant decrease in recovery upon stressing, this is not the case for pertuzumab. Since the selected signature peptides have been shown to be stable under stress conditions[13] (Bults et al., unpublished data), it is likely that binding to affimer T11 is affected due to modification of the binding site or a change in conformation affecting binding. It is known that trastuzumab is susceptible to numerous modifications, namely to deamidation at Asn-30 in the light chain, at Asn-55 in the heavy chain and isomerization of Asp-102 in the heavy chain.[12] A loss of binding to anti-idiotypic antibodies, as used in a commercially available sandwich ELISA for trastuzumab, has been observed upon deamidation of Asn-55.[13] Notably, isomerization of Asp-102 was shown to result in an almost complete loss of antiproliferative activity against a breast cancer cell line in culture, indicating that binding sites to HER2 or conformational changes that are necessary for activity are affected. Detailed analysis by cation-exchange chromatography showed that stressing trastuzumab at 37 °C in PBS at pH 7.4[38] resulted in numerous modified forms, while this was much less pronounced in the case of pertuzumab.[39] Further research is needed to elucidate the reasons for a reduced recovery of trastuzumab from plasma upon stressing also in view of using Affimer reagents for bioanalytical assays in clinical samples.

CONCLUSIONS

We have developed a bead-based Affimer reagent method for the enrichment of trastuzumab and pertuzumab from human plasma at clinically relevant concentrations. Affimers were immobilized through their 6-His-tag to Ni^{2+} beads or via a unique Cys residue to maleimide beads. As part of this work, we developed a rapid screening method based on microtiter plate-based enrichment followed by LC−MS analysis in the SRM mode based on previous work by Klont et al.[20] It is interesting to note that only about 2% or less of either target antibody is enriched from plasma using microtiter plates due to the small surface area (see Table S2, Supporting Information). This is important as many analytical immunoaffinity enrichment methods (e.g., ELISAs) may capture only 1−2% of the target analyte depending on its concentration in the sample and the amount of antibody on the microtiter plate surface. This may create a bias toward high-affinity binders and thus may not give a true representation of the mixture of proteoforms of the target protein in the sample.

An important aspect of method development was to achieve a high, reproducible recovery. Protein digestion and notably the release of the signature peptide that was used for the SRM assay proved to be a limiting factor for trastuzumab, while this was less of a problem for pertuzumab. To arrive at reproducibly high recoveries for both antibodies, we screened a number of denaturants and surfactants resulting in the use of 0.5% sodium deoxycholate as an optimal additive, giving recoveries of more than 70% for trastuzumab and pertuzumab. It is also advantageous that sodium deoxycholate can be removed by acid precipitation prior to LC−MS analysis.

We observed a reduction in recovery after stressing trastuzumab at 37 °C (PBS, pH 7.4) for up to 3 weeks, while this was not the case for pertuzumab. As such conditions may also occur in patients during treatment, our observations are relevant in light of isolating proteoforms of these therapeutic antibodies from patient plasma to study in vivo biotransformation. The ability to use different Affimer reagents targeting different binding sites on trastuzumab is of interest in this context, as it may allow capturing of a wider range of proteoforms. Work along this line is currently ongoing.

The low unspecific binding of affimer−maleimide beads to plasma proteins (see Figure S2, Supporting Information) is encouraging for the application to clinical samples since it ensures that sufficient amounts of both therapeutic antibodies can be captured for further analysis, with little or no interference from plasma proteins.

ASSOCIATED CONTENT

Supporting Information

The Supporting Information is available free of charge at https://pubs.acs.org/doi/10.1021/acs.analchem.1c02807.

Calculation of percentage recovery for trastuzumab and pertuzumab based on the ratio between the released signature peptides and the added stable-isotope-labeled internal standard peptides (Table S1); prioritization of antitrastuzumab and antipertuzumab Affimer reagents using a microtiter plate-based binding assay and LC−MS in the SRM mode as readout (Figure S1); analysis of the enriched fraction from the Ni^{2+} and the maleimide beads by SDS polyacrylamide gel electrophoresis of trastuzumab and pertuzumab (Figure S2); evaluation of the four prioritized antitrastuzumab affimers T11, T6, T12, and T15 (Figure S3); evaluation of the effect of different denaturing conditions during on-bead trypsin digestion on the recovery of trastuzumab and pertuzumab (Figure S4); and BLASTp sequence alignment of light (a) and heavy chains (b) of trastuzumab (Query) and pertuzumab (Sbjct) (Figure S5) (PDF)

Percentage recovery obtained using the plate-based enrichment method (Table S2) (XLSL)

AUTHOR INFORMATION

Corresponding Author

Rainer Bischoff − *Department of Analytical Biochemistry, Groningen Research Institute of Pharmacy, University of Groningen, 9713 AV Groningen, The Netherlands;* orcid.org/0000-0001-9849-0121; Email: r.p.h.bischoff@rug.nl

Authors

Oladapo Olaleye − *Department of Analytical Biochemistry, Groningen Research Institute of Pharmacy, University of Groningen, 9713 AV Groningen, The Netherlands*

https://doi.org/10.1021/acs.analchem.1c02807
Anal. Chem. 2021, 93, 13597−13605

Baubek Spanov − *Department of Analytical Biochemistry, Groningen Research Institute of Pharmacy, University of Groningen, 9713 AV Groningen, The Netherlands*
Robert Ford − *Avacta Life Sciences Limited, Wetherby LS23 7FA, United Kingdom*
Natalia Govorukhina − *Department of Analytical Biochemistry, Groningen Research Institute of Pharmacy, University of Groningen, 9713 AV Groningen, The Netherlands*
Nico C. van de Merbel − *Department of Analytical Biochemistry, Groningen Research Institute of Pharmacy, University of Groningen, 9713 AV Groningen, The Netherlands; Bioanalytical Laboratory, PRA Health Sciences, Early Development Services, Assen 9407 TK, The Netherlands*

Complete contact information is available at: https://pubs.acs.org/10.1021/acs.analchem.1c02807

Notes

The authors declare no competing financial interest.

■ ACKNOWLEDGMENTS

B.S. and O.O. are funded by a grant of the European Commission (H2020 MSCA-ITN 2017 "Analytics for Biologics", grant agreement ID 765502).

■ REFERENCES

(1) Scheuer, W.; Friess, T.; Burtscher, H.; Bossenmaier, B.; Endl, J.; Hasmann, M. *Cancer Res.* **2009**, *69*, 9330−9336.
(2) Swain, S. M.; Baselga, J.; Kim, S.-B.; Ro, J.; Semiglazov, V.; Campone, M.; Ciruelos, E.; Ferrero, J.-M.; Schneeweiss, A.; Heeson, S.; Clark, E.; Ross, G.; Benyunes, M. C.; Cortés, J. *N. Engl. J. Med.* **2015**, *372*, 724−734.
(3) von Minckwitz, G.; Procter, M.; de Azambuja, E.; Zardavas, D.; Benyunes, M.; Viale, G.; Suter, T.; Arahmani, A.; Rouchet, N.; Clark, E.; Knott, A.; Lang, I.; Levy, C.; Yardley, D. A.; Bines, J.; Gelber, R. D.; Piccart, M.; Baselga, J. *N. Engl. J. Med.* **2017**, *377*, 122−131.
(4) He, X.-Y.; Xu, Z.; Melrose, J.; Mullowney, A.; Vasquez, M.; Queen, C.; Vexler, V.; Klingbeil, C.; Co, M. S.; Berg, E. L. *J. Immunol.* **1998**, *160*, 1029.
(5) Gemmete, J. J.; Mukherji, S. K. *Am. J. Neuroradiol.* **2011**, *32*, 1373−1374.
(6) Gerratana, L.; Bonotto, M.; Bozza, C.; Ongaro, E.; Fanotto, V.; Pelizzari, G.; Puglisi, F. *Expert Opin. Biol. Ther.* **2017**, *17*, 365−374.
(7) Hudis, C. A. *N. Engl. J. Med.* **2007**, *357*, 39−51.
(8) Tóth, G.; Szöőr, Á.; Simon, L.; Yarden, Y.; Szöllősi, J.; Vereb, G. *MAbs* **2016**, *8*, 1361−1370.
(9) Yang, N.; Tang, Q.; Hu, P.; Lewis, M. J. *Anal. Chem.* **2018**, *90*, 7896−7902.
(10) Yao, M.; Chen, B.; Zhao, W.; Mehl, J. T.; Li, L.; Zhu, M. *Drug Metab. Dispos.* **2018**, *46*, 451−457.
(11) Huang, L.; Lu, J.; Wroblewski, V. J.; Beals, J. M.; Riggin, R. M. *Anal. Chem.* **2005**, *77*, 1432−1439.
(12) Harris, R. J.; Kabakoff, B.; Macchi, F. D.; Shen, F. J.; Kwong, M.; Andya, J. D.; Shire, S. J.; Bjork, N.; Totpal, K.; Chen, A. B. *J. Chromatogr. B: Biomed. Sci. Appl.* **2001**, *752*, 233−245.
(13) Bults, P.; Bischoff, R.; Bakker, H.; Gietema, J. A.; van de Merbel, N. C. *Anal. Chem.* **2016**, *88*, 1871−1877.
(14) Aswad, D. W.; Paranandi, M. V.; Schurter, B. T. *J. Pharm. Biomed. Anal.* **2000**, *21*, 1129−1136.
(15) Bischoff, R.; Kolbe, H. V. *J. Chromatogr. B: Biomed. Sci. Appl.* **1994**, *662*, 261−278.
(16) Geiger, T.; Clarke, S. *J. Biol. Chem.* **1987**, *262*, 785−794.
(17) Fang, X.; Zhang, W.-W. *J. Proteomics* **2008**, *71*, 284−303.
(18) Fung, E. N.; Bryan, P.; Kozhich, A. *Bioanalysis* **2016**, *8*, 847−856.
(19) Boström, T.; Johansson, H. J.; Lehtio, J.; Uhlen, M.; Hober, S. *J. Proteome Res.* **2014**, *13*, 4424−4435.
(20) Klont, F.; Hadderingh, M.; Horvatovich, P.; Ten Hacken, N. H. T.; Bischoff, R. *J. Proteome Res.* **2018**, *17*, 2892−2899.
(21) Yu, X.; Yang, Y.-P.; Dikici, E.; Deo, S. K.; Daunert, S. *Annu. Rev. Anal. Chem.* **2017**, *10*, 293−320.
(22) Crivianu-Gaita, V.; Thompson, M. *Biosens. Bioelectron.* **2016**, *85*, 32−45.
(23) Kyle, S. *Trends Biochem. Sci.* **2018**, *43*, 230−232.
(24) Adamson, H.; Nicholl, A.; Tiede, C.; Tang, A. A.; Davidson, A.; Curd, H.; Wignall, A.; Ford, R.; Nuttall, J.; McPherson, M. J.; Johnson, M.; Tomlinson, D. C. *Biotechniques* **2019**, *67*, 261−269.
(25) Arrata, I.; Barnard, A.; Tomlinson, D. C.; Wilson, A. J. *Chem. Commun.* **2017**, *53*, 2834−2837.
(26) Lopata, A.; Hughes, R.; Tiede, C.; Heissler, S. M.; Sellers, J. R.; Knight, P. J.; Tomlinson, D.; Peckham, M. *Sci. Rep.* **2018**, *8*, No. 6572.
(27) Robinson, J. I.; Baxter, E. W.; Owen, R. L.; Thomsen, M.; Tomlinson, D. C.; Waterhouse, M. P.; Win, S. J.; Nettleship, J. E.; Tiede, C.; Foster, R. J.; Owens, R. J.; Fishwick, C. W. G.; Harris, S. A.; Goldman, A.; McPherson, M. J.; Morgan, A. W. *Proc. Natl. Acad. Sci. U.S.A.* **2018**, *115*, E72−E81.
(28) Tiede, C.; Bedford, R.; Heseltine, S. J.; Smith, G.; Wijetunga, I.; Ross, R.; AlQallaf, D.; Roberts, A. P. E.; Balls, A.; Curd, A.; Hughes, R. E.; Martin, H.; Needham, S. R.; Zanetti-Domingues, L. C.; Sadigh, Y.; Peacock, T. P.; Tang, A. A.; Gibson, N.; Kyle, H.; Platt, G. W.; Ingram, N.; Taylor, T.; Coletta, L. P.; Manfield, I.; Knowles, M.; Bell, S.; Esteves, F.; Maqbool, A.; Prasad, R. K.; Drinkhill, M.; Bon, R. S.; Patel, V.; Goodchild, S. A.; Martin-Fernandez, M.; Owens, R. J.; Nettleship, J. E.; Webb, M. E.; Harrison, M.; Lippiat, J. D.; Ponnambalam, S.; Peckham, M.; Smith, A.; Ferrigno, P. K.; Johnson, M.; McPherson, M. J.; Tomlinson, D. C. *eLife* **2017**, *6*, No. e24903.
(29) Xie, C.; Tiede, C.; Zhang, X.; Wang, C.; Li, Z.; Xu, X.; McPherson, M. J.; Tomlinson, D. C.; Xu, W. *Sci. Rep.* **2017**, *7*, No. 9608.
(30) Wishart, D. S.; Feunang, Y. D.; Guo, A. C.; Lo, E. J.; Marcu, A.; Grant, J. R.; Sajed, T.; Johnson, D.; Li, C.; Sayeeda, Z.; Assempour, N.; Iynkkaran, I.; Liu, Y.; Maciejewski, A.; Gale, N.; Wilson, A.; Chin, L.; Cummings, R.; Le, D.; Pon, A.; Knox, C.; Wilson, M. *Nucleic Acids Res.* **2018**, *46*, D1074−D1082.
(31) Strohalm, M.; Hassman, M.; Košata, B.; Kodíček, M. *Rapid Commun. Mass Spectrom.* **2008**, *22*, 905−908.
(32) Altschul, S. F.; Gish, W.; Miller, W.; Myers, E. W.; Lipman, D. J. *J. Mol. Biol.* **1990**, *215*, 403−410.
(33) Fuentes, G.; Scaltriti, M.; Baselga, J.; Verma, C. S. *Breast Cancer Res.* **2011**, *13*, No. R54.
(34) Lua, W.-H.; Gan, S. K.-E.; Lane, D. P.; Verma, C. S. *npj Breast Cancer* **2015**, *1*, No. 15012.
(35) Hustoft, H.; Malerod, H.; Wilson, S.; Reubsaet, L.; Lundanes, E.; Greibrokk, T. *A Critical Review of Trypsin Digestion for LC-MS Based Proteomics*; IntechOpen, 2012.
(36) Yu, Y. Q.; Gilar, M. *RapiGest SF Surfactant: An Enabling Tool for in -Solution Enzymatic Protein Digestions*; Waters Corporation: Boston, MA, 2009.
(37) Zhou, J.; Zhou, T.; Cao, R.; Liu, Z.; Shen, J.; Chen, P.; Wang, X.; Liang, S. *J. Proteome Res.* **2006**, *5*, 2547−2553.
(38) Schmid, I.; Bonnington, L.; Gerl, M.; Bomans, K.; Thaller, A. L.; Wagner, K.; Schlothauer, T.; Falkenstein, R.; Zimmermann, B.; Kopitz, J.; Hasmann, M.; Bauss, F.; Haberger, M.; Reusch, D.; Bulau, P. *Commun. Biol.* **2018**, *1*, No. 28.
(39) Spanov, B.; Olaleye, O.; Lingg, N.; Bentlage, A. E. H.; Govorukhina, N.; Hermans, J.; van de Merbel, N.; Vidarsson, G.; Jungbauer, A.; Bischoff, R. *J. Chromatogr. A* **2021**, *1655*, 462506.